Environment and Natural Resources Journal

Volume 23
Issue 5
2025

Groundwater Studies for Sustaining Peatlands against Fire Disasters and Supporting Water Resources

David Andrio[1,3*], Nur Islami[2], and Lita Darmayanti[1]

[1]*Environmental Engineering, Universitas Riau, Pekanbaru, Indonesia*
[2]*Physics Education, Universitas Riau, Pekanbaru, Indonesia*
[3]*Center for Technology and Energy Application, Universitas Riau, Pekanbaru, Indonesia*

ARTICLE INFO

Received: 2 Jan 2025
Received in revised: 15 May 2025
Accepted: 29 May 2025
Published online: 2 Jul 2025
DOI: 10.32526/ennrj/23/20250002

Keywords:
Peat fire/ Peatland/ Geoelectrical Resistivity

*** Corresponding author:**
E-mail:
davidandrio@lecturer.unri.ac.id

ABSTRACT

There are two main issues related to water resources in coastal areas covered by peat soil. The first problem is peat fires, which occur during the dry season and are difficult to extinguish because the characteristics of peat make it very flammable. The second problem is a lack of clean water resources for the needs of the surrounding community. This study investigates the feasibility of groundwater potential for prevention of peat fire tragedies, and groundwater resources for community use. This study employed an integrated approach that combined geoelectrical resistivity surveys with physical and chemical analyses of soil and groundwater to assess groundwater potential both as a water resource and as a preventive measure against peatland fires. The results of this study indicated that all groundwater samples were contaminated with seawater and exceeded the permissible limits set by the World Health Organization (WHO), making them unsuitable for human consumption. Except for the central and eastern parts of the study area, peat soil exhibited resistivity values ranging from 30 to 210 Ω·m, largely influenced by its fluid and clay content. Through interpretation of resistivity data, variations in sand and gravel content at different depths were identified. Shallow aquifers were present at a depth of 10 meters in the south and 12 meters in the north, and the peat soil had a thickness that varied up to 4 meters. Thus while the groundwater reserves in the study area are not fit for community use or consumption, they do appear sufficient to significantly reduce the risk of widespread peat fire disasters.

1. INTRODUCTION

Water is one of the most vital natural resources required by all living organisms and for maintaining environmental sustainability. Water quality in a region can be influenced by natural environmental factors as well as anthropogenic activities, including negligence, which may lead to in the contamination of water sources (Karunanidhi et al., 2021). Moreover, water plays a crucial role in maintaining the hydrological balance of peatlands, which is, which is essential for ensuring the long-term sustainability of peat ecosystems (Tanneberger et al., 2021). In peatland areas, shallow groundwater is often unsuitable for suitable for daily human use, as it is inevitably contaminated by the peat material itself (Dettmann et al., 2021; Szczepański et al., 2021). Near surface peat soil also dries out easily during the dry, making peatlands more prone to drought and increasingly susceptible to fire (Nelson et al., 2021; Taufik et al., 2022). Peat fires cause severe damage to both the ecosystems living in peat areas and the surrounding environment, especially through the production of hazardous smoke and haze.

Peatland fires can exhibit a wide temporal range and may smolder underground, persisting for extended periods. Extinguishing peat fires requires a very tiring effort, because most peatlands in remote areas and difficult to reach. Peat soil frequently experiences fire disasters during the dry season (Kurniawan et al., 2024; Rezanezhad et al., 2016). Typically, peat fires

Citation: Andrio D, Islami N, Darmayanti L. Groundwater studies for sustaining peatlands against fire disasters and supporting water resources. Environ. Nat. Resour. J. 2025;23(5):420-435. (https://doi.org/10.32526/ennrj/23/20250002)

are uncontrollable due to the large volume water needed to extinguish them. To effectively prevent sub-surface fires, it is essential to fully saturate the peat soil with water, beyond merely extinguishing surface flames. Research on peat soil has been documented in a number of studies. To preserve wet environment, Ghit et al. (2018) conducted research to the area of peat soil in Algeria. Crowson et al. (2019) mapped Sumatra Island's peat forests using satellite remote sensing fusion. In contrast, Chasmer et al. (2017) used Lidar data to measure the thickness of peat soil and the quantity lost due to peat fires. To preserve peat soil, Zak and McInnes (2022) carried out wetting of peatlands to maintain ecological conditions. The restoration of peatlands can help counteract detrimental impacts and deliver advantages for both local and global communities related to carbon, water, biodiversity, and human well-being (Farrell et al., 2024).

Silvestri et al. (2019) reported the application of geophysical techniques in the study of peat soil and how to compare aerial geophysics topographic method for determining the depth of peat soil measured from the surface. Several studies have reported their findings on the application of geophysical techniques to investigate groundwater characteristics, peat properties and potential, seawater intrusion in shallow aquifers, subsurface void, and even hydrothermal systems in hilly regions (Islami et al., 2025; Tajul Baharuddin et al., 2013; Islami, 2018; Islami et al., 2019). Taufik et al. (2022) developed the PFVI index for assessing fire risk in tropical peatlands, incorporating information on groundwater tables and groundwater retention. This PFVI index can be used as a peat fire risk management tool, and its application can minimize the risk of fire in tropical peatlands.

The amount of water needed for extinguishing fires in peatlands is significantly greater than in other forest fire cases. Utilizing local groundwater as a resource for firefighting could help address these major challenges more effectively. This study uses a combination of geoelectrical resistivity of soil and groundwater physical analysis to examine the potential of groundwater and peatland in the research area. Thus, it can be a foundation for the peat to protect it from fire hazards can cause disasters to the environment and also human life. The findings of this study should be useful in informing the local community and government about environmental factors that should be considered when allocating the peatland's water resources, and it also does not rule out the possibility of providing references for research in other parts of the world with the same case. With regard to the accessibility and utilization of water resources for the prompt containment of forest fires, particularly in the peatland region, this research is very significant for providing protection for peatlands from fires, it will contribute to climate resilience, sustainable peatland management and the long-term sustainability of the peat environment.

2. METHODOLOGY

2.1 The study area

The study was conducted in the eastern part of the central Sumatra Basin (Figure 1), Riau Province, Indonesia, which is the largest tertiary sedimentary basin in the country and a key source of hydrocarbons. In terms of its tectonic context, the region is classified as a back-arc basin, which primarily influences its geological characteristics. Peat soil is dominant on the surface, especially in the area near the coast (Zhao et al., 2022). Peat soil, wherever it is located, is very prone to burning during the dry season (Nelson et al., 2021). This situation is particularly alarming because nearly all of Indonesia's peatland areas have undergone changes in function for agricultural purposes (Juniyanti et al., 2021; Purwanto et al., 2020).

2.2 Methodology

In this study, an analysis of peat and soil characteristics, groundwater characteristics, and the relationship between electrical resistivity and the characteristics of the measured material was carried out.

2.2.1 Analysis of soil properties

Fourteen soil samples were gathered from various sites where the geoelectrical resistivity data survey was conducted. In order to improve our understanding of the properties of the soil in the study region, soil grain size was examined (Guo, 2009). To describe the original soil, a soil sample was taken at a depth of roughly 40-50 cm. A well was bored to obtain soil samples of subterranean soil at different depths in addition to the near-surface dirt. Sixteen soil samples of dirt were collected at certain depths. The dried soil was sieved and categorized based on the grain size classification system of Braja (2019) to obtain information on the soil's moisture content.

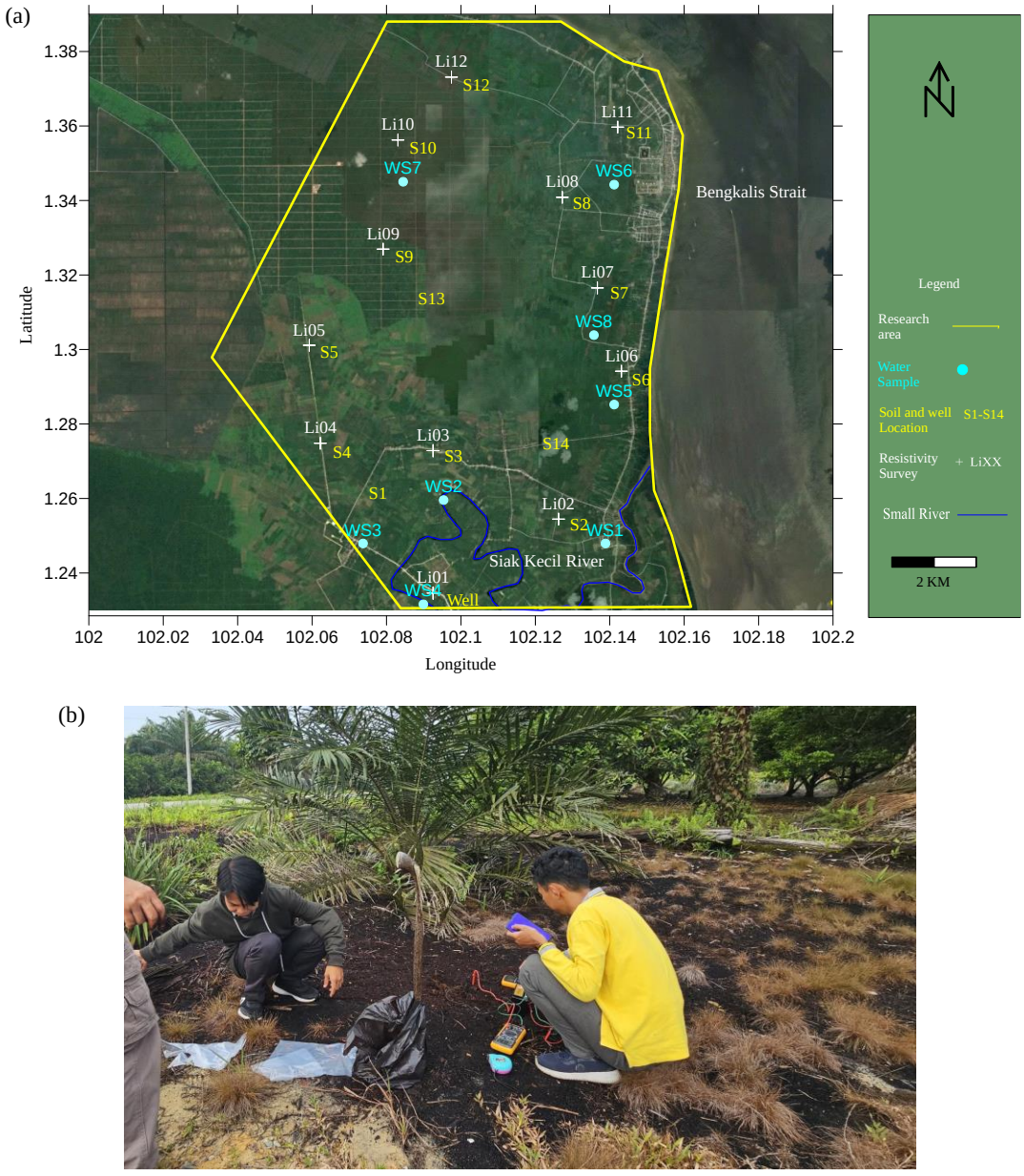

Figure 1. (a) Map of study area, (b) peatland condition in the study site

2.2.2 Measuring soil resistivity directly

At various locations near the resistivity survey, fifty direct readings of soil resistivity measurements were completed. To determine the genuine resistivity values of specific places of interest, direct measurements of soil resistivity were obtained for various soil environments and conditions, such as wet clay, dried clay, dry peat, and others. To find the genuine resistivity values, a Wenner setup with a narrow electrode spacing of 5 cm was employed. According to Telford et al. (1990), it is possible to determine the accurate resistivity value of the soil by measuring it with a reasonably small electrode directly, with the assumption that the soil is homogenous for small electrode spacing. At the measuring site, the type and color of the soil were noted and samples of the surface soil were collected to examine the grain size.

2.2.3 Chemical examination of groundwater

Six existing boreholes were used to gather groundwater samples, as shown in Figure 1. There were eight water samples taken. The paucity of existing wells in the research area made it challenging to gather groundwater samples at the same target zone depths. Based on information provided by the well owner, all of the current wells are deeper than 50 meters, with the exception of W5, a dig well, which is only about 5 meters deep. The wells' deepest point was where the well screen was positioned.

Regretfully, the well's owner could not recall the well's precise depth. Furthermore, because the wells were sealed with concrete, it was not possible to estimate the depth to the water's surface. The characteristics of the groundwater were investigated using a chemical examination of the water. Since the deeper aquifer is the primary supply of residential water, special attention has been paid to it. A peristaltic pump was used to gather groundwater samples. A number of in-situ characteristics were measured, including temperature, salinity, pH, total dissolved solids (TDS), water level, and well depth. Four hundred milliliters of water were sampled and stored in plastic bottles. Standard techniques were used to analyze each and every water sample (Clesceri et al., 1999). The water samples were transported to the Chemical Analysis Laboratory for less than 30 hours while being kept at a temperature of about 4°C in a thermos. There, they were analyzed for ion content using Ion Chromatography (IC) and Inductively Coupled Plasma (ICP), which is the latest method offering higher sensitivity, speed, and precision (Appelo and Postma, 2004).

2.2.4 Geoelectrical resistivity survey

Figure 1 shows all the locations where 1D geoelectrical resistivity surveys were conducted. At these sites, 12 traverse lines with lengths of between 200 and 260 meters were established using the Schlumberger configuration. This configuration was chosen due to its greater depth of investigation, less time and a high signal to noise ratio (Telford et al., 1990). A custom resistivity meter with a varied maximum output current and DC voltage was used. The amount of space in the field determined how long the survey would take. To improve the resolution of shallower layers, comparatively small 0.5 m increments in electrode spacing were employed for the first 10 measurements.

The apparent resistivity value was computed using the unprocessed field data, which included electric current, voltage, and electrode spacing. The actual subsurface resistivity value was then obtained by entering these data into the Res1D program for the inversion stage (Loke, 2001). The early model utilized in the data processing was the baseline for the initial data. The first set of data came from interpreting the trend line that the raw data's apparent resistivity had produced. Next, each geoelectrical layer's resistivity value and thickness were calculated using the Res1D software. In order to obtain the true resistivity value, both forward and inverse modeling techniques were used in the process. To compare with the measured value in forward modeling, the program computes the value of theoretical resistivity in the model created by repetitive inversion. The resistivity curve's layered-ground model, which represented the likelihood (expressed in terms of least squares) of corresponding to the field curves, was determined by inverse modeling. Finally, the data was mapped and contoured using Surfer 8.02 (Golden Software).

3. RESULTS AND DISCUSSION

3.1 Characteristics of the soil and a direct assessment of its resistivity

Table 1 shows the type of soil and resistivity measurement. The interpretation of subsurface resistivity was guided by these findings. The data given in Table 1 shows that the resistivity value of saturated peat soil will depend on the clay content in the peat pore. The magnitude of peat resistivity increases if the peat content increases. When peat is mixed with clay, the magnitude of resistivity will decrease as the clay content mixed with the peat increases. Peat without clay content shows a resistivity value of 195-210 Ω·m for wet conditions, and for relatively dry conditions it is 70-95 Ω·m. According to Basri et al. (2019), the pore fluid in the peat soil determines the peat resistance value especially in dry conditions. As the moisture content drops, the medium's ability to conduct current generally diminishes because of empty pores. For this reason, the resistivity value typically rises. Even though the medium in Table 1 was filled with water, the coarse sand was made of the electric current-resistant quartz crystal. This increased the medium's overall conductivity because the water in the pores served as a conductor to transfer electrical current.

3.2 Groundwater chemical analysis

The results of chemical analysis of groundwater samples from both the recently drilled well and the existing wells are presented in Table 2. The final rows of the table show the World Health Organization's (WHO, 2008) maximum concentration that suitable for human consumption. With the exception of WS5 and WS8 (5.68 and 5.91, respectively), the majority of water samples have pH values between 6 and 8 (not safe for human consumption). All groundwater samples have K, Ca, Mg, and Na cation levels that are within the permissible range for ingestion by humans. Furthermore, the SO_4^{-2} anion content was

comparatively low (<400 mg/L), making it safe for ingestion by humans. With the exception of WS3 and WS7, the Fe anion's content is unfit for human consumption which is more than 0.3 mg/L. The elevated seawater concentration but decreased pH content in the groundwater samples from these two wells is most likely the cause of the lower content of Fe. The organic content of the water is what causes the fluctuation in pH (Hounslow, 1995). Table 2 shows differences in the cation content, particularly in Fe, which are higher than the typical threshold for human intake that is safe.

Table 1. Actual resistivity readings of the drilled well's surface soil and soil sample

No	Type of soil	Soil sources	Number of samples	Colour	Resistivity range (Ω·m)	
					Wet condition (Moisture content >25%)	Dry condition (Moisture content<10%)
1	Peat (100%)	Near surface	5	Dark grey	70.33-95.6	195.2-210.6
2	Peat (50%-75%)	Near surface	5	Dark grey	40.3-55.6	78.6-98.3
3	Peat (25%-50%)	Near surface	4	Dark grey	31.4-36.2	80.7-89.1
4	Clay	New well	4	Dark grey	16.5-23.4	61.7-73.4
5	Clay	New well	4	Relatively white	55.3-67.4	241.2-269.3
6	Medium to fine Sand	New well	4	Relatively white, (fully saturated)	46.5-68.2	-
7	Coarse sand	New well	4	Relatively white, (fully saturated)	51.2-84.5	-

Table 2. Chemical content of the groundwater sample

Well name	pH	Salinity (0/00)	TDS (mg/L)	Cl (mg/L)	SO_4 (mg/L)	K (mg/L)	Ca (mg/L)	Mg (mg/L)	Na (mg/L)	Fe (mg/L)
WS1	7.12	0.73	2,270.7	834.75	291	1.93	42.6	35.69	55.86	0.23
WS2	7.36	1.13	3,060.2	1,189.25	273.4	2.33	72.3	48.19	67.36	0.34
WS3	7.18	0.54	2,100.8	634.85	292	1.72	32.8	35.67	55.84	0.16
WS4	6.87	0.82	2,050.2	517.5	382.4	1.88	38.1	27.57	39.13	3.16
WS5	5.68	0	163.4	63.3	124.8	1.24	14.4	3.23	22.18	2.73
WS6	6.92	0.22	1,092.3	276.5	368.6	1.53	44.7	21.43	10.25	5.83
WS7	6.97	0.31	1,130.6	411.3	317.4	1.68	36.5	17.52	37.12	2.22
WS8	5.91	0.21	1,102.4	306.6	378.6	1.72	47.8	19.44	17.24	6.82
WHO	6-8			250	400			150	200	0.3

The anion concentration of the water sample reveals that all of the water samples have comparatively greater chloride ion values than the 250 mg/L (human consumption limit) except WS5. The well WS5 location is relatively far from the coast and is the cause of the low concentration of chloride ion. A map showing TDS and chloride is shown in Figure 2. Circles indicate groundwater chloride concentrations, which are comparatively low in the southern portion of the research region. In the northern portion of the research region, they are, nevertheless, comparatively high. The north of the research region has higher chloride concentrations, which are related to its closeness to the coastline. In water samples that are quite close to the coastline, other researchers have also discovered relatively high concentrations of chloride (Telahigue et al., 2018; Ayed et al., 2018). For TDS, the same pattern was noted. All of the water in the aquifer, though, is thought to be a combination of freshly arrived non-brackish water and seawater that was previously trapped there.

In Figure 2, the chloride ions are plotted against other ions for all the water samples from the research area. Based on the plotted graph in Figure 2, it can be concluded that the groundwater comes from the same saltwater source. Chemical reactions like ion exchange activities or mixing can alter the chemical makeup of fresh groundwater. In reality, the data match those shown in Table 2. As seen in Figure 3, most ions generally exhibit a strong association with the chloride ions. In the deeper aquifer, K, Mg, and Na ions have a strong association with chloride, with the exception of Ca ions. This suggests that the source of these ions is the same saline water (Kim et al., 2003).

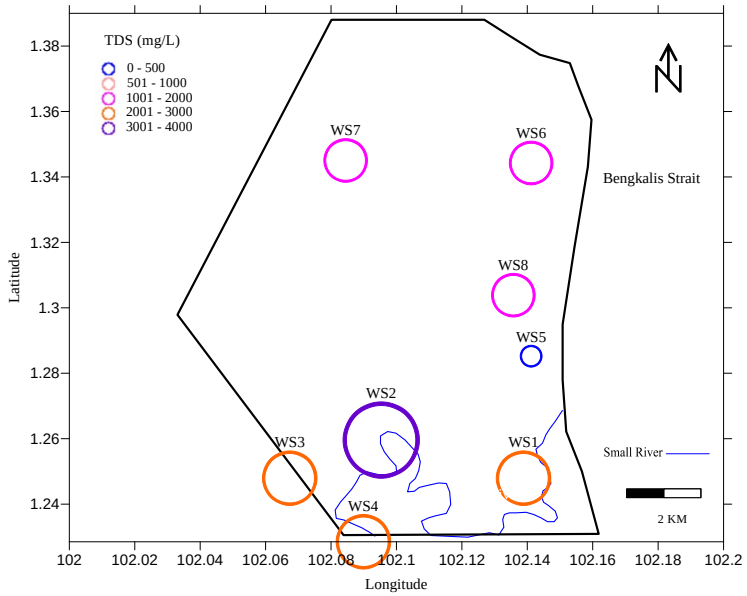

Figure 2. TDS distribution in the research area

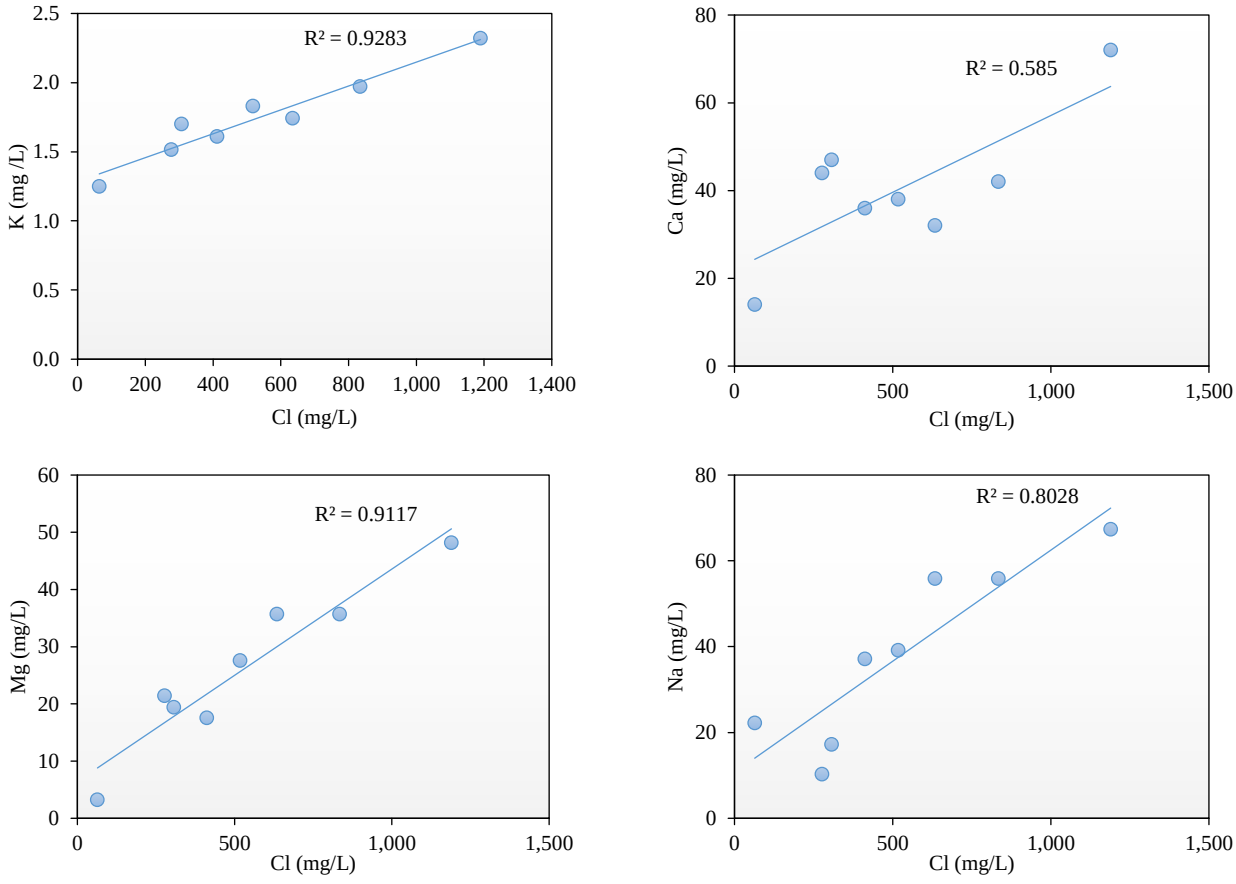

Figure 3. Scatter plot of Cl versus other anion content

3.3 Data from well-drilled

In order to acquire geological information for the purpose of calibrating and interpreting the resistivity data, a fresh well was dug approximately in the middle of the research region. Soil samples were collected during the drilling of the well. In order to get geological data for this study region, several researchers also took soil samples while digging (Zhuo et al., 2017; Li et al., 2019). The soil analysis findings are plotted against depth in Figure 4. There is clay soil, which is light grey, down to around two meters. A notable change in clay color to grey occurs

from 2 to 12 meters. Deeper than 12 to 19 meters is where fine sand can be found. During the site survey, the first aquifer was discovered in this depth range. At 52 meters below the surface, a second aquifer with fine-grained sand was discovered. The well's maximum depth was 70 meters, and coarse sand is found between 58 and 70 meters (Figure 4).

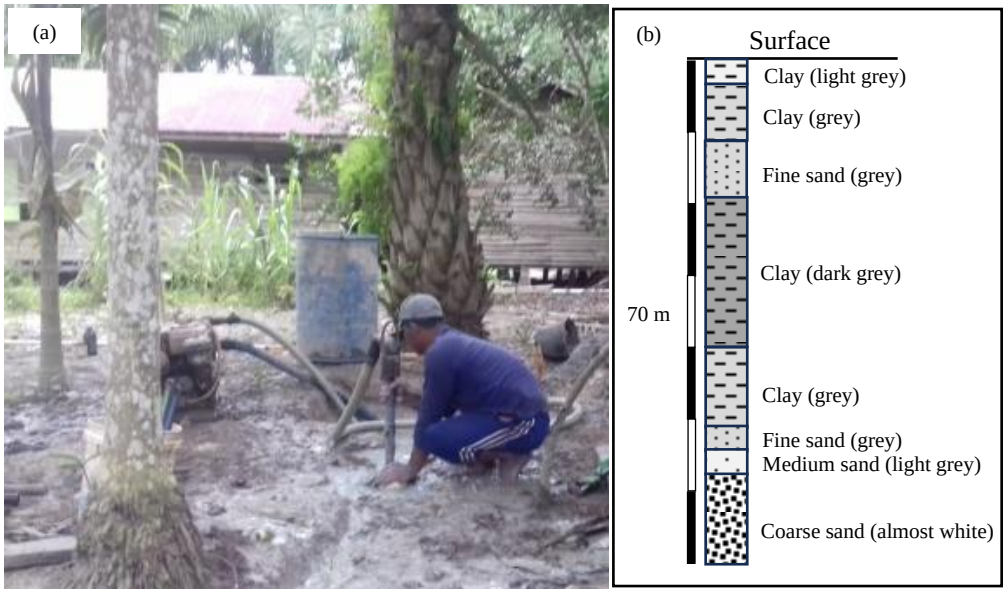

Figure 4. Well drilling photograph (a) and Lithology log (b)

3.4 Interpretation of resistivity below the surface

All the resistivity data were processed using Res1DInv to estimate the depth of each layer and true resistivity value of each layer. The inversion process was carried out using resistivity raw data collected from the field. The subsurface's geoelectrical resistivity for each site is interpreted in Figure 5. The result of the inversion shows the resistivity model that is represented by the block form in the picture, the computed apparent resistivity is displayed using a curve line and then the observed apparent resistivity data are shown by using the plus (+) sign.

Direct soil resistivity measurement in Table 1 for certain soil conditions was utilized as a guide during the interpretation process to interpret the subsurface resistivity (Figure 5). The direct resistivity measurement of the soil is also supported by well log data that was obtained from the drilled well (Figure 4). The different types of curves for the span from the top surface to the second aquifer were recognized in Figure 5. Res1D was used to process the geoelectrical resistivity curves with an RMS error of less than 5% for all line surveys. Similar types of resistivity undulation are seen in these twelve resistivity curves model. With the exception of the LS6 and LS7 lines, which have resistivities of about 150 Ω·m. In the near surface layer, resistivity data ranges from 30 to 50 Ω·m which shows layers of peat mixed with clay that are indicated by near-surface resistivity range from 30 to 50 Ω·m. A resistivity of about 150 Ω·m. indicates that there is rather dry clay present. Direct field observations made near each survey site substantiate this. The geoelectrical resistivity curve's form provides an indicator of lithology interchange, as seen in the following pattern. The rock formation and lithology in the study area are indicated by five distinct types of geoelectrical resistivity curves. This conclusion is based on the characteristic of block and guided by the lithology data. They are peat soil followed by clay, then layered by the first aquifer, and clay layer between the first and second aquifers, and the second aquifer. Nevertheless, the eastern and middle regions of the research area did not contain peat soil. This is the opposite of what was found in the resistivity study of LS6 and LS7, where the top surface had a resistivity value of roughly 150 Ω·m. The lithology information gleaned from the drilling procedure also lends credence to this hypothesis (Figure 4).

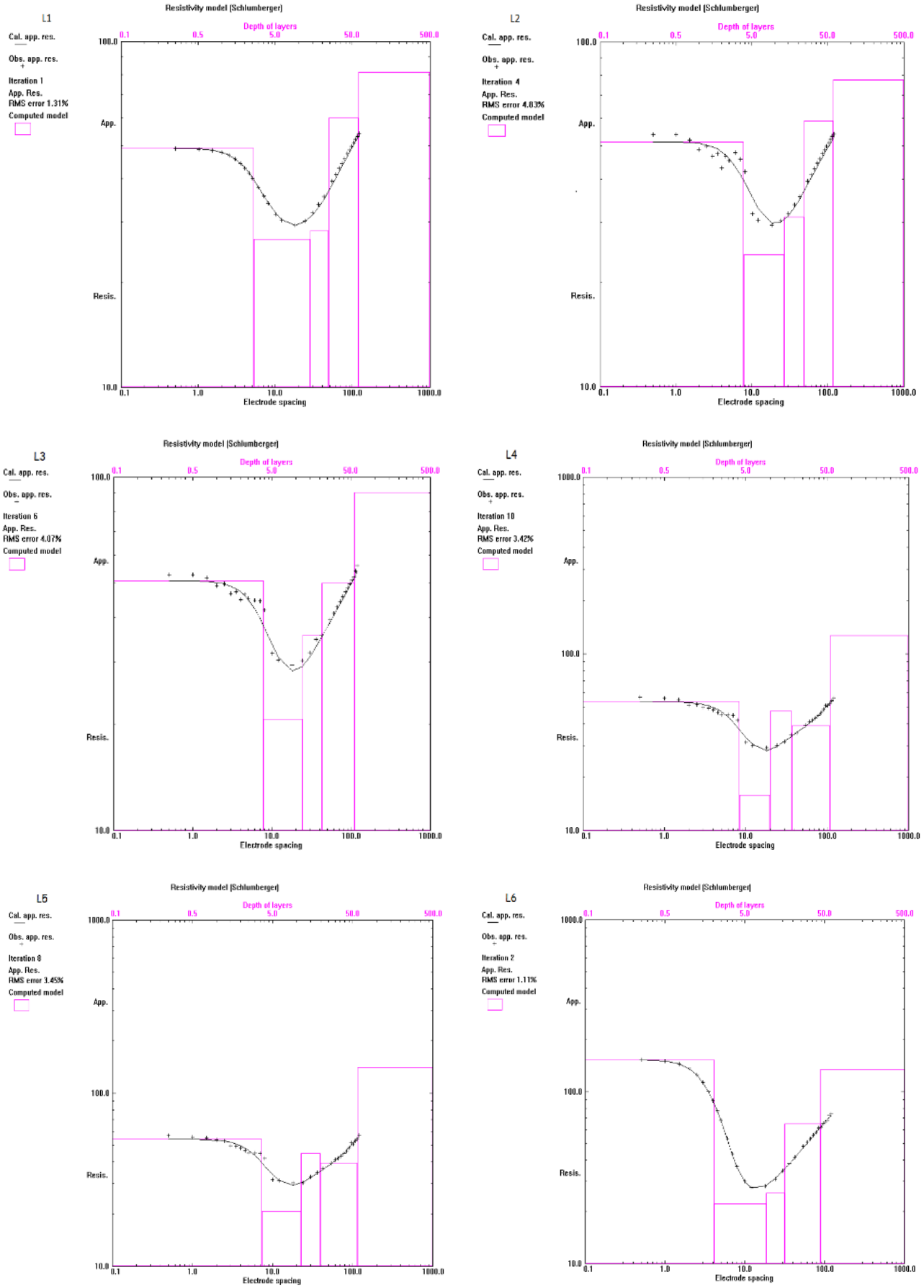

Figure 5. The resistivity plotted against depth

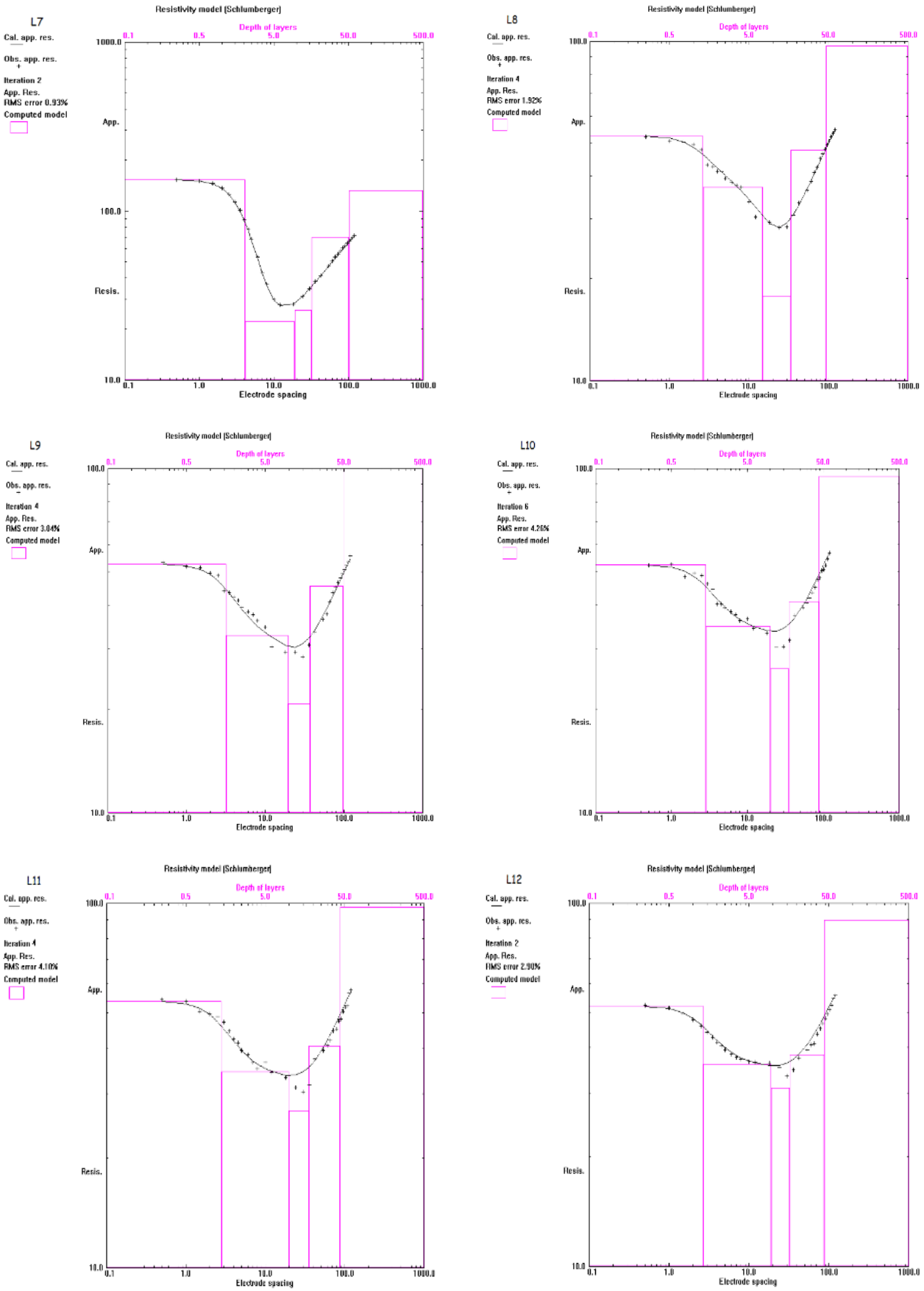

Figure 5. The resistivity plotted against depth (cont.)

In the southern portion of the research area (LS9, LS10, LS11, LS12, LS13, and LS14), the value of the resistivity data was found to be around 50 Ω·m from the surface down to a depth of 1.5 m based on the interpretation of the resistivity data in Figure 5. This resistivity value is consistent with the peat soil, which was determined by direct resistivity testing and ranged from 47 to 54 Ω·m (Table 1). In the northern portion (LS1, LS3, and LS4), the peat soil resistivity values range from 48 to 53 Ω·m, indicating a relatively thick peat layer averaging 2.60 m. As seen in the LS7 and eastern portions as well (LS5 and LS6), no peat soil was discovered in the middle of the research area. The resistivity value in these locations is 150 Ω·m, or dried clay soil, close to the surface. The following layer has a resistivity of 22 to 35 Ω·m, which is indicative of saturated clay soil. Because the north portion of this stratum was closer to the beach, there was a comparatively greater resistivity difference between it and the south. Out of all the layers, the third layer has the lowest resistance (25-38 Ω·m). This suggests that the layer on top of it is an aquifer that is full of brackish water. This aquifer gets deeper as it moves northward. This aquifer gets deeper as it moves northward. Nonetheless, this aquifer's resistivity rises toward the south, suggesting that the groundwater's brackishness gradually diminishes as one moves landward. Beneath the first aquifer lies a clay layer with resistivity between 50 and 59 Ω·m. The resistivity values of the deepest layer, which matches to the second aquifer, range from 80 to 120 Ω·m. In the deeper depth, the second aquifer is located at a depth of roughly 60 meters in the north and 40 meters in the south. The fresh aquifer has comparatively less chlorides and sulphates in the groundwater in the southern portion, and these kinds progressively rise in the direction of the north, according to the relatively large resistivity difference in the second aquifer.

The resistivity distribution in the subsurface is displayed in Figure 6. The resistivity readings were utilized to contour it laterally using a kriging method. The kriging spreading was based on a variogram modelled with a lag distance of 0.056 (unit is in degree) for individually depth below the surface (0 m). The resistivity distribution at the surface is comparatively higher (>120 Ω·m) in the middle and eastern regions of the research area. Peat soil was represented by the dark grey zone. The resistivity value is typically about 25 Ω·m at depths of 10 and 20 m, indicating the presence of a brackish water zone in the first aquifer. The clay zone was grey at 30, 40, and 50 meters below the surface. The second aquifer, which is light blue in hue, is the last stratum.

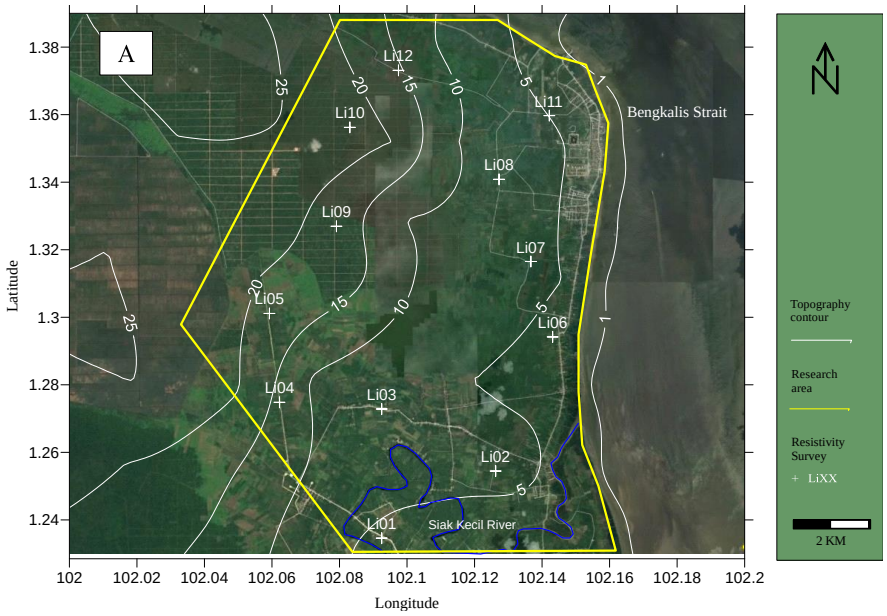

Figure 6. Topography map (a) and distribution of resistivity value at the surface to -60 m depth (b-h)

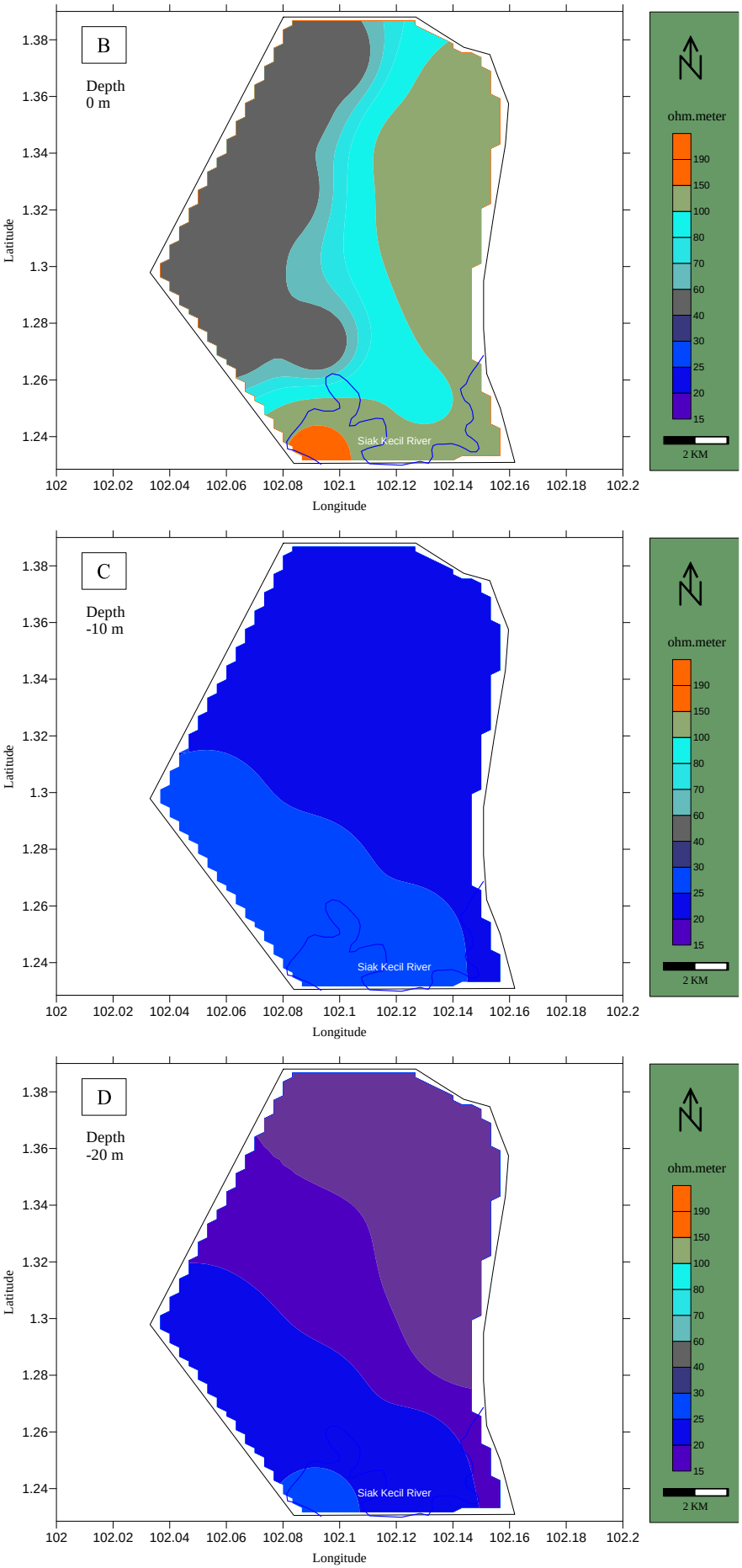

Figure 6. Topography map (a) and distribution of resistivity value at the surface to -60 m depth (b-h) (cont.)

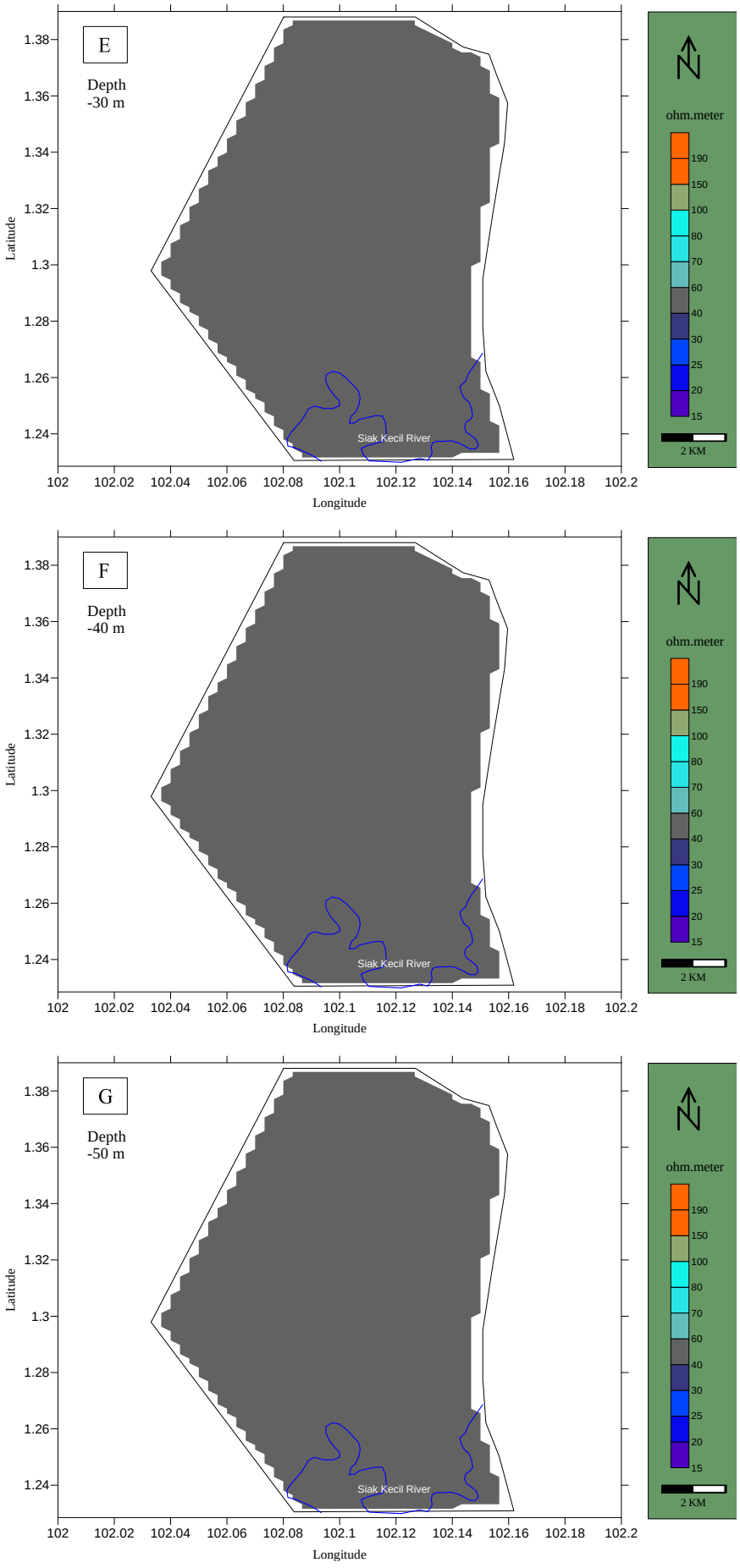

Figure 6. Topography map (a) and distribution of resistivity value at the surface to -60 m depth (b-h) (cont.)

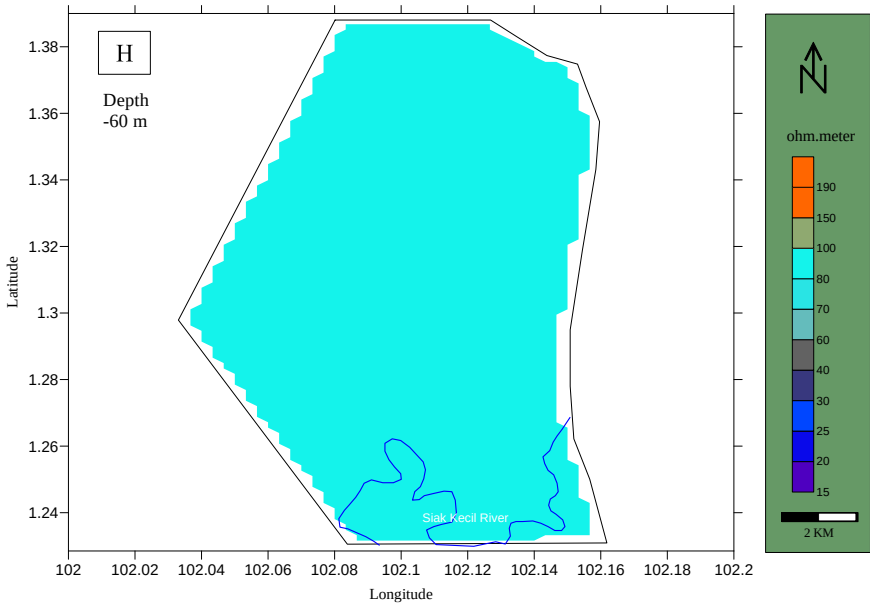

Figure 6. Topography map (a) and distribution of resistivity value at the surface to -60 m depth (b-h) (cont.)

3.5 Anticipation for prevent Peat fire disaster

Based on the resistivity data interpretation, the thickness of peat soil was estimated for all the research area. These data's trends show that resistivity changes dramatically at a depth of roughly two meters. This suggests that the soil had changed from being peat to becoming clay. In contrast, the southern region of the research area experiences no such change. This suggests that in the southern part of the research area, the peat soil is not found in the near surface (0-3 m deep). The reason these zones don't have peat soil is because the Siak River overflowed and inundated their surface, leaving clay as the predominant material covering these places.

The total bounded study area is 1.88×10^8 m^2 which is used in the estimation peat and aquifer volume. The peat's thickness ranges from 0 m in the southern area but is found to be about 4 m thick in the northern area, with an average thickness of roughly 2 m. The depth of peatland is according to the geoelectrical resistivity interpretation for the entire region. Figure 7 displays the soil thickness that is only 4 m thick in the north portion. Other studies indicate that peat thickness varies from 1 meter to tens of meters, depending on the depositional environment during peat formation (Crezee et al., 2022; Islami and Irianti, 2021; Anda et al., 2021; Islami et al., 2023). Finally, the total volume of the peat soil within the study area is about 3.72×10^8 m^3. This volume prognosis is based on the boundary of the countering and the depth in each location. Peat porosity in this region is about 41% (Sutejoa et al., 2016), and then the peat,s total pore volume can reach about 1.54×10^8 m^3.

In order to do early anticipation of the peat fire disaster, the need of water is important to investigate. The thickness of the first aquifer as determined by interpreting the resistivity data depicted in Figure 8 is roughly 8 m thick in the south region. The aquifer is thicker just about 12.8 m thick in the north region. Because thickness is not recorded uniformly, the increase in thickness from the south to the middle area is less than the increase in thickness from the middle to the northern area; therefore, the first aquifer's thickness does not increase gradually to the north. Since the first aquifer has an average thickness of 10.2 meters, the approximate total volume of water resources in the pores with average porosity of 30% in the shallow aquifer is predicted to be as much as 5.75×10^8 m^3.

The overall amount of water in the reservoir of the shallow aquifer is expected to be greater than what would be required to plug all of the peat soil pores, which helps to prevent peat fire disasters. Because the peat soil has significantly high of porosity and permeability (Sutejoa et al., 2016), water can naturally seep to the bottom part of the material of the pores in the peat. To put it another way, all of the water in the first aquifer can be used to predict the amount of water needed to avoid a peat fire. This eliminates the need for helicopters to carry water to other sites, which has historically been the method used when peat fires occur.

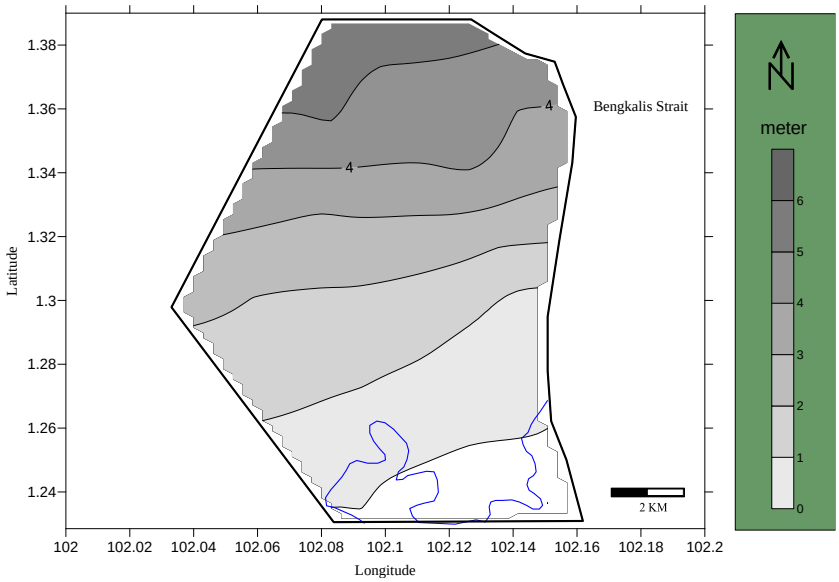

Figure 7. Thickness of peat soil obtained from the resistivity interpretation

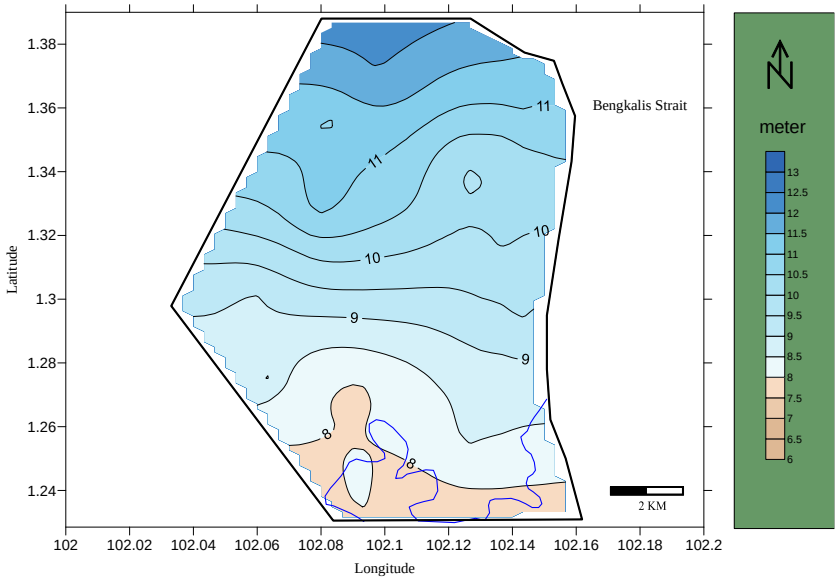

Figure 8. Thickness of the first aquifer

Finally, according to a volume analysis of both peat soil and groundwater, the water resources from the first aquifer are quite feasible to supply water in this area to put out flames of the peat in the dry season. But if peat fires occurred in this area or perhaps in other locations of peatlands, the issue that can come up is that it is quite challenging to get the fire site in order to drill wells during a fire. Therefore, in the event of a drought, it would be wise to locate wells with automated pumps in case of peat fires. This would reduce the likelihood of a peat fire happening. In addition, the automated pumps would keep the peat's moisture content constant. Ultimately, it will maintain the peat wetland area's ecosystem's viability.

3.6 Future discussion

This study shows a snapshot of groundwater chemistry and resistivity but does not consider how seasonal variability may impact groundwater availability or quality for fire prevention. Future research should focus on how changes between the dry and wet seasons can affect important factors such as groundwater levels, salinity concentrations, and peat moisture dynamics in coastal areas. Multi-seasonal studies using long-term field monitoring approaches, hydrological modeling, and satellite imagery would be very useful in understanding the complex interactions between seasonal rainfall, seawater intrusion, and groundwater balance. Particular attention should be

paid to the impacts of prolonged dry seasons or extreme wet seasons on peat drying, increased oxidation, subsidence, and changes in groundwater and surface water quality. The study conducted by Ahmad shows the importance of maintaining the condition of peatlands from fires. They did this engaging with the community about how important it is to maintain the condition of peatlands.

4. CONCLUSION

The findings of this study suggest that the peat soil and aquifer conditions in the study area can be effectively investigated using the geoelectrical resistivity method. Direct surface resistivity measurement is a highly helpful tool for resistivity data interpretation and calibration. The north of the research area has rather brackish groundwater, as evidenced by the comparatively high chloride concentration of the water samples. According to the resistivity data interpretation, the study region is made up of coarse sand, clay, and peat soil. Based on the distribution of resistivity values, it was possible to detect and map the depths of the two aquifers and the peat. The research area's middle and eastern regions have no peat soil, and the thickness of the soil varies. The entire volume of water in the shallow aquifer appears to be more than sufficient to prevent a peat fire calamity in the future, even as the aquifer's depth grows toward the north.

REFERENCES

Anda M, Ritung S, Suryani E, Hikmat M, Yatno E, Mulyani A, et al. Revisiting tropical peatlands in Indonesia: Semi-detailed mapping, extent and depth distribution assessment. Geoderma 2021;402:Article No. 115235.

Appelo CA, Postma D. Geochemistry, Groundwater and Pollution. London: CRC press; 2004.

Ayed B, Jmal I, Sahal S, Bouri S. The seawater intrusion assessment in coastal aquifers using GALDIT method and groundwater quality index: The Djeffara of Medenine coastal aquifer (Southeastern Tunisia). Arabian Journal of Geosciences 2018;11(20):Article No. 609.

Basri K, Wahab N, Talib MK, Zainorabidin A. Sub-surface profiling using electrical resistivity tomography (ERT) with complement from peat sampler. Civil Engineering and Architecture 2019;7(6A):7-18.

Braja MD. Advanced Soil Mechanics. 4th ed. London: CRC Press; 2019.

Chasmer LE, Hopkinson CD, Petrone RM, Sitar M. Using multitemporal and multispectral airborne lidar to assess depth of peat loss and correspondence with a new active normalized burn ratio for wildfires. Geophysical Research Letters 2017;44(23):11,851-9.

Clesceri LS, Greenberg AE, Eaton AD. Standard Methods for the Examination of Water and Wastewater. Washington DC: APHA; 1999.

Crezee B, Dargie GC, Ewango CE, Mitchard ET, Emba BO, Kanyama TJ, et al. Mapping peat thickness and carbon stocks of the central Congo Basin using field data. Nature Geoscience 2022;15(8):639-44.

Crowson M, Warren-Thomas E, Hill JK, Hariyadi B, Agus F, Saad A, et al. A comparison of satellite remote sensing data fusion methods to map peat swamp forest loss in Sumatra, Indonesia. Remote Sensing in Ecology and Conservation 2019;5(3):247-58.

Dettmann U, Kraft NN, Rech R, Heidkamp A, Tiemeyer B. Analysis of peat soil organic carbon, total nitrogen, soil water content and basal respiration: Is there a 'best' drying temperature? Geoderma 2021;403:Article No. 115231.

Farrell CA, Connolly J, Morley TR. Charting a course for peatland restoration in Ireland: A case study to support restoration frameworks in other regions. Restoration Ecology 2024;32(7):e14216.

Ghit K, Muller S, Bélair GD, Belouahem Abed D, Daoud-Bouattour A, Benslama M. Palaeoecological significance and conservation of peat-forming wetlands of Algeria. Revue d'Écologie (La Terre et La Vie) 2018;73(4):414-30.

Guo M. Soil sampling and methods of analysis. Journal of Environmental Quality 2009;38(1):Article No. 375.

Hounslow A. Water Quality Data: Analysis and Interpretation. Boca Raton: CRC Press; 2018.

Islami N, Irianti M, Fakhruddin F, Zulirfan Z. A preliminary study of geothermal resources in the Rokan Hulu Regency, Riau, Indonesia. Journal of Physics: Conference Series 2019;1185(1):Article No. 012003.

Islami N, Irianti M, Yusoff I. An effective method for quantitative interpretation of seawater intrusion in shallow aquifers from electrical resistivity data. Current Applied Science and Technology 2025;25(1):1-14.

Islami N, Irianti M. A quantitative interpretation of salt water mixture in the shallow aquifer through the geoelectrical resistivity data. Journal of Physics: Conference Series 2023;2582(1):Article No. 012001.

Islami N, Irianti M. Resistivity characteristics of soil saturated with variation of salt water-fresh water mixture. Journal of Physics: Conference Series 2021;2049(1):Article No. 012029.

Islami N. Groundwater exploration in the bedrock area using geoelectrical resistivity survey. IOP Conference Series: Earth and Environmental Science 2018;186(3):Article No. 012016.

Juniyanti L, Purnomo H, Kartodihardjo H, Prasetyo LB. Understanding the driving forces and actors of land change due to forestry and agricultural practices in sumatra and kalimantan: A systematic review. Land 2021;10(5):Article No. 463.

Karunanidhi D, Aravinthasamy P, Deepali M, Subramani T, Shankar K. Groundwater pollution and human health risks in an industrialized region of southern India: Impacts of the COVID-19 lockdown and the monsoon seasonal cycles. Archives of Environmental Contamination and Toxicology 2021;80(1):259-76.

Kim Y, Lee KS, Koh DC, Lee DH, Lee SG, Park WB, et al. Hydrogeochemical and isotopic evidence of groundwater salinization in a coastal aquifer: A case study in Jeju volcanic island, Korea. Journal of Hydrology 2003;270(3-4):282-94.

Kurniawan A, Graham LB, Applegate G, Arifanti VB, Akbar A, Hadi EE, et al. Impacts of rainfall on peat fire during the dry season and wet dry season on degraded tropical peatland in South Sumatra, Indonesia. IOP Conference Series: Earth and Environmental Science 2024;1315(1):Article No. 012060.

Li S, Huang Z, Zhao K, Xu H, Fang Q. Comparative analysis of pit deformation characteristics in typical region soft soil deposits of China. Arabian Journal of Geosciences 2019;12:1-11.

Loke MH. Tutorial: 2-D and 3-D Electrical Imaging Surveys [internet]. 2001 [cited 2024 March 10]. Available from: http://www.geoelectrical.com.

Nelson K, Thompson D, Hopkinson C, Petrone R, Chasmer L. Peatland-fire interactions: A review of wildland fire feedbacks and interactions in Canadian boreal peatlands. Science of the Total Environment 2021;769:Article No. 145212.

Purwanto E, Santoso H, Jelsma I, Widayati A, Nugroho HY, van Noordwijk M. Agroforestry as policy option for forest-zone oil palm production in Indonesia. Land 2020;9(12):Article No. 531.

Rezanezhad F, Price JS, Quinton WL, Lennartz B, Milojevic T, Van Cappellen P. Structure of peat soils and implications for water storage, flow and solute transport: A review update for geochemists. Chemical Geology 2016;429:75-84.

Silvestri S, Knight R, Viezzoli A, Richardson CJ, Anshari GZ, Dewar N, et al. Quantification of peat thickness and stored carbon at the landscape scale in tropical peatlands: A comparison of airborne geophysics and an empirical topographic method. Journal of Geophysical Research: Earth Surface 2019;124(12):3107-23.

Sutejoa Y, Dewi R, Hastuti Y, Rustam RK. Engineering properties of peat in Ogan ilir regency. Jurnal Teknologi (Sciences & Engineering) 2016;78(7-3):61-9.

Szczepański M, Szajdak LW, Meysner T. Impact of shelterbelt and peatland barriers on agricultural landscape groundwater: Carbon and nitrogen compounds removal efficiency. Agronomy 2021;11(10):Article No. 1972.

Tajul Baharuddin MF, Taib S, Hashim R, Abidin MH, Rahman NI. Assessment of seawater intrusion to the agricultural sustainability at the coastal area of Carey Island, Selangor, Malaysia. Arabian Journal of Geosciences 2013;6(1):3909-28.

Tanneberger F, Appulo L, Ewert S, Lakner S, Ó Brolcháin N, Peters J, et al. The power of nature-based solutions: How peatlands can help us to achieve key EU sustainability objectives. Advanced Sustainable Systems 2021;5(1):Article No. 2000146.

Taufik M, Widyastuti MT, Sulaiman A, Murdiyarso D, Santikayasa IP, Minasny B. An improved drought-fire assessment for managing fire risks in tropical peatlands. Agricultural and Forest Meteorology 2022;312:Article No. 108738.

Telahigue F, Agoubi B, Souid F, Kharroubi A. Assessment of seawater intrusion in an arid coastal aquifer, south-eastern Tunisia, using multivariate statistical analysis and chloride mass balance. Physics and Chemistry of the Earth, Parts A/B/C 2018;106:37-46.

Telford WM, Geldart LP, Sheriff RE. Applied Geophysics. Cambridge University Press; 1990.

World Health Organisation (WHO). WHO Guidelines for Drinking-Water Quality. 3rd ed. Geneva: WHO; 2008.

Zak D, McInnes RJ. A call for refining the peatland restoration strategy in Europe. Journal of Applied Ecology 2022;59(11):2698-704.

Zhao J, Lee JS, Elmore AJ, Fatimah YA, Numata I, Zhang X, et al. Spatial patterns and drivers of smallholder oil palm expansion within peat swamp forests of Riau, Indonesia. Environmental Research Letters 2022;17(4):Article No. 044015.

Zhuo L, Han D, Dai Q. Exploration of empirical relationship between surface soil temperature and surface soil moisture over two catchments of contrasting climates and land covers. Arabian Journal of Geosciences 2017;10:1-11.